

Flow-induced flapping of thin flexible plates

Mario Pistis¹, Victor A. Eremeyev², Giorgio Fotia³, Antonio Cazzani⁴

Department of Civil and Environmental Engineering and Architecture (DICAAR), University of Cagliari, Via Marengo 2 09123 Cagliari (CA), Italy

¹Corresponding author

E-mail: ¹mario.pistis@unica.it, ²victor.ereyev@unica.it, ³giorgio.fotia@unica.it,

⁴antonio.cazzani@unica.it

Received 17 March 2026; accepted 12 April 2026; published online 22 April 2026
DOI <https://doi.org/10.21595/vp.2026.26407>



75th International Conference on Vibroengineering in Trieste, Italy, April 13, 2026

Copyright © 2026 Mario Pistis, et al. This is an open access article distributed under the Creative Commons Attribution License, which permits unrestricted use, distribution, and reproduction in any medium, provided the original work is properly cited.

Abstract. The behavior of highly flexible structures under Flow-Induced Vibrations (FIV) conditions, in certain flow regimes, is characterized by a strong coupling between the structural dynamics and fluid phenomena such as vortex shedding. This work presents selected results of ongoing research aimed at developing a fully open-source numerical framework to simulate the dynamic behavior of such structures immersed in complex fluid flows. The framework is based on a partitioned coupling approach of a fluid solver and a structural one, an Arbitrary Lagrangian-Eulerian mesh motion strategy, and Quasi-Newton Interface stabilization technique (IQN) that accounts for large displacements of the coupling interface. To illustrate the potential of such framework, we present strongly coupled Fluid-Structure Interaction (FSI) simulations of a thin flexible elastic plate subjected to FIV.

Keywords: fluid structure interaction, flow induced vibrations, computational fluid dynamics, computational structural mechanics, multiphysics simulation.

1. Introduction

Fluid-Structure Interaction involving highly flexible structures is a significant issue in Civil, Mechanical, Biomedical and Ocean Engineering, where the mutual coupling between flow and structural deformation affects their dynamic response [1]. Thin plates immersed in a fluid flow are a classical example of this class of problems because they exhibit large displacements, material nonlinearities, and strong sensitivity to the interaction between fluid loads and structural mechanics [2]. These features make them a useful reference problem for the development and assessment of numerical strategies for strongly coupled FSI.

A reliable numerical description of such systems is important for several emerging applications, including bioinspired materials and devices, energy harvesting from fluid flows, and lightweight flexible structures, such as pneumatic systems and submerged components in Ocean Engineering [3]. In literature numerous relevant contributions on these topics can be found, e. g. [4], including studies on flapping structures [5], partitioned and monolithic coupling schemes [6], Immersed and Embedded Boundary Methods (IBM/EBM) [7] and advanced interface-coupling treatments, such as isogeometric analysis [8], which maintain physical consistency and achieve high accuracy with reduced computational cost even with non-matching meshes. However, many of the available implementations rely on software environments which are not easily accessible.

The added value of the present work lies in the development of a fully open-source, modular, and reproducible framework that combines established Computational Fluid Dynamics (CFD) and Computational Structural Mechanics (CSM) solvers within a strongly coupled strategy suitable for highly flexible structures undergoing large displacements. The proposed environment is intended to serve as an open tool for the analysis of such structures immersed in fluid flow and as a basis for further developments toward high fidelity engineering applications.

With the aim of illustrating the potential of this approach, we focus on the numerical modeling of a flexible plate immersed in a parallel flow [9] and show the main components required to

address this class of problems, including the governing equations, the coupling strategy, and the relevant parameters used in the simulations. The paper is organized as follows: in Section 2 the governing equations for the solid and fluid domains, together with the coupling models, are presented. Section 3 describes the details of the problem under investigation. Section 4 reports the results. Finally, Section 5 provides some conclusions.

2. Governing equations

The fundamental partial differential equations that govern the fluid and structural fields are briefly introduced, thereby establishing the theoretical foundation for the coupled simulation approach. Specifically, the incompressible Navier-Stokes equations describe the fluid flow, while the structural response is modeled using nonlinear elasticity theory. Finally, the mesh motion is handled within an Arbitrary Lagrangian-Eulerian approach.

2.1. Fluid domain

The incompressible fluid dynamics is governed by the unsteady Navier-Stokes equations, which express the conservation of mass, Eq. (1), and linear momentum, Eq. (2), for a Newtonian fluid. These equations can be mathematically represented as:

$$\nabla \cdot \dot{\mathbf{u}} = 0, \quad (1)$$

$$\frac{\partial \dot{\mathbf{u}}}{\partial t} + \nabla \cdot (\dot{\mathbf{u}}\dot{\mathbf{u}}) - \nabla \cdot \mathbf{R} = -\nabla \frac{p}{\rho_f} + \mathbf{S}_u, \quad (2)$$

where, t is the time, $\dot{\mathbf{u}}$ is the fluid velocity vector, p is the pressure, ρ_f is the fluid density, \mathbf{R} is the Reynolds stress tensor, and \mathbf{S}_u is the external momentum source of the fluid. Eq. (1), i.e. the continuity equation, constrains the velocity field to ensure mass conservation within the (incompressible) fluid domain. Furthermore no-slip boundary condition is enforced at the fluid-structure interface to ensure kinematic continuity. In this work, the numerical solution of these equations employs a Finite Volume Method, as implemented in OpenFOAM v. 2312 [10], which discretizes the domain into control volumes and integrates the governing equations over these volumes, providing a robust framework for the simulation of complex fluid flows.

2.2. Structural domain

The structural domain, particularly for the case of highly flexible solids such as plates, requires a robust formulation capable of capturing large deformations, that can be addressed through a nonlinear Finite Element Method (FEM). The equation to be solved are the nonlinear dynamic equilibrium equations, expressed as Cauchy's first equation of motion Eq. (3), which is expressed in a Lagrangian framework to capture the large-deformation behavior of the structure:

$$\rho_s \ddot{\mathbf{u}} = \nabla \cdot \boldsymbol{\sigma} + \mathbf{f}, \quad (3)$$

where, ρ_s is the structural density, $\ddot{\mathbf{u}}$ is the structural acceleration vector, $\boldsymbol{\sigma}$ is the Cauchy stress tensor, and \mathbf{f} is the external force vector. These are solved using CalculiX v. 2.20 [11], which implements a Finite Element formulation of dynamic equilibrium expressed in a total Lagrangian framework for large deformation analysis. In the present work, CalculiX employs a displacement-based Finite Element Method, where the spatial discretization of the structural domain is performed, and the equations are solved using an implicit time integration scheme. This approach allows for an accurate representation of geometric nonlinearities inherent in large structural displacements while maintaining computational efficiency.

2.3. Coupling strategy

To perform the simulation within the described numerical framework, the two separate solvers, i.e. OpenFOAM and CalculiX, are coupled for the fluid and the structural domains, respectively. The coupling is handled via the PreCICE library v. 2404 [12] and the adapters for the two solvers, as illustrated in Fig. 1.

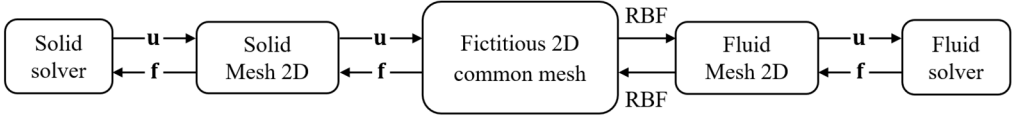


Fig. 1. Coupling scheme was implemented in PreCICE. The common fictitious 2D interface is where the quantities are projected; RBF refers to radial basis function

In this setup, forces and displacements are exchanged across a 2D fictitious interface mesh. The fluid solver transfers a traction vector resulting from the viscous and pressure stress to the structural solver as external loads, while the structural solver transfers the displacements back to the fluid solver. The information exchange occurs within an iterative loop until convergence is reached at each time step, according to a parallel implicit coupling scheme, where the two solvers are executed simultaneously within each coupling iteration. Mesh motion is computed using the displacement–Laplacian approach described by Eq. (4):

$$\nabla \cdot (\gamma \nabla \mathbf{u}) = \mathbf{0}, \quad (4)$$

where a quadratic inverse-distance d diffusivity from the fluid-structure interface, $\gamma \propto 1/d^2$, is chosen, ensuring smooth propagation of the structural displacements into the fluid domain.

The partitioned FSI coupling is stabilized and accelerated through an Interface Quasi-Newton method with Inverse Least Squares (IQN-ILS), which provides an approximation of the interface Jacobian based on the previous solutions, thus mitigating added-mass instabilities.

3. Methods

We consider a Fluid-Structure Interaction problem (see Fig. 2) of a clamped plate whose length is L and thickness h , subjected to an incoming laminar flow having a vertical velocity U_∞ . Thickness-to-length ratio is set to $h/L = 1/40$, bending rigidity, Eq. (5), is $R_1 = 0.0125$ and structure-to-fluid mass ratio, Eq. (6), is $R_2 = 75$. Reynolds number, Eq. (7), is $Re = 20$:

$$R_1 = \frac{Eh^3}{12(1 - \nu_s^2)\rho_f U_\infty^2 L^3}, \quad (5)$$

$$R_2 = \frac{\rho_s h}{\rho_f L}, \quad (6)$$

$$Re = \frac{U_\infty L}{\nu_f}, \quad (7)$$

where E and ν_s are, respectively, Young’s modulus and Poisson’s ratio of the structural material and ν_f is the kinematic viscosity of the fluid. The computational domain has a length $5L$, a width $6L$, and a depth L , as shown in Fig. 2. The mesh is extended in the X - Y plane and extruded in the Z direction. It is structured and uniform, and made of hexahedral cells for both structure and fluid. A preliminary mesh convergence study (Table 1) was carried out by considering three different mesh resolutions of the fluid domain (see Fig. 7) while the Structural Mesh (SM) is always the same. Three different Fluid Meshes (FM) are analyzed: FM1, FM2 and FM3. Each mesh is obtained from the previous one through successive refinement, as shown in Fig. 7(a)-(b). The

finest mesh FM3 has $\Delta x_{FM3} = L/128$, the medium mesh FM2 has $\Delta x_{FM2} = L/64$, and the coarsest mesh FM1 has $\Delta x_{FM1} = L/32$. For every mesh, a time step Δt is employed to keep the Courant-Friedrichs-Lewy number, $CFL < 1$, Eq. (8), ensuring both numerical stability and solution accuracy:

$$CFL = \frac{U_\infty \Delta t}{\Delta x}. \quad (8)$$

With regard to the IQN-ILS coupling parameters, a tolerance $e_{FSI} = 10^{-3}$ was adopted for the partitioned FSI solution, with a maximum number of iterations $N_{max} = 300$ and an Initial Relaxation Factor $IRF = 0.5$. The mapping of forces and displacements onto the fictitious exchange mesh is performed using polynomial Radial Basis Functions with a radius $R_{RBF} = L$.

Table 1. Mesh description of the structural mesh SM and fluid meshes FM1, FM2 and FM3. Here, C_L and C_D are the resulting lift and drag coefficient, respectively

| Solid mesh | | | |
|------------|--------------------|--------|--------|
| SM | Elements | 244 | |
| | Nodes | 1470 | |
| Fluid mesh | | | |
| Mesh | Cells $X \times Y$ | C_D | C_L |
| FM1 | 98×84 | 1.2110 | 1.6639 |
| FM2 | 194×168 | 1.1376 | 1.5895 |
| FM3 | 388×336 | 1.1347 | 1.5865 |

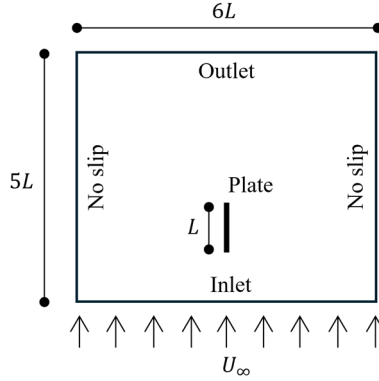


Fig. 2. Computational domain and boundary conditions sketch

4. Results

The results of the numerical simulations are presented. The behavior of the plate is analyzed via the transverse, x , and streamwise, y , displacements of the plate tip, as well as the drag and lift coefficients, C_D and C_L , defined in Eq. (9-10):

$$C_D = \frac{|\mathbf{F}_D|}{0.5\rho_f U_\infty^2 A}, \quad \mathbf{F}_D = \rho_f \sum_i A_i \mathbf{n}_i (p_i - p_r), \quad (9)$$

$$C_L = \frac{|\mathbf{F}_L|}{0.5\rho_f U_\infty^2 A}, \quad \mathbf{F}_L = \mu_f \sum_i A_i \cdot \mathbf{R}_d. \quad (10)$$

where A is the surface area, p_r the reference pressure, μ_f the fluid dynamic viscosity and \mathbf{R}_d the deviatoric component of the Reynolds stress tensor \mathbf{R} . Summation on all surfaces, A_i , whose pressure value is p_i and normal vector \mathbf{n}_i , produces the resultant forces. Convergence analysis is

based on residuals associated to quantities of interest, such as C_D , C_L , \mathbf{u} , and computed as:

$$e_{\blacksquare} = \frac{|\blacksquare - \blacksquare_{pr}|}{\blacksquare_{ref}}, \quad (11)$$

where, \blacksquare represents the considered quantity, \blacksquare_{pr} the value of \blacksquare computed using the previous mesh definition and \blacksquare_{ref} the corresponding reference value, computed, in this case, using finest mesh FM3. Fig. 3 illustrates the outcome of this study, with reference to C_L . Similar results are obtained for all other quantities. Based on this study of convergence, we adopt the latter mesh.

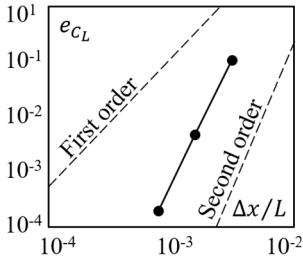


Fig. 3. Residual of C_L for increasing mesh resolutions

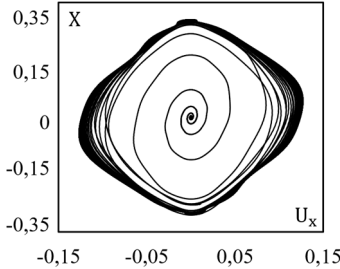


Fig. 4. Phase portrait of the tip plate displacements

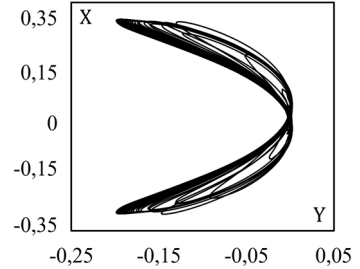


Fig. 5. Motion diagram of the tip plate displacements

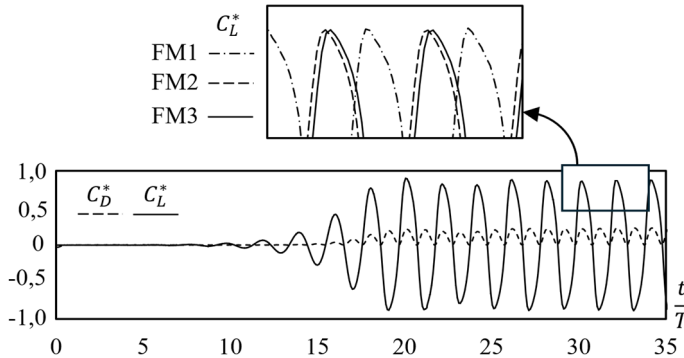


Fig. 6. Time histories of drag and lift coefficients C_D^* and C_L^* respect to the flapping times of the plate. C_D^* is translated and aligned with the horizontal axis. The detail shows the solution for all meshes



Fig. 7. $0.2L \times 0.2L$ mesh box detail for the plate tip

Under the assumed set of parameters, the thin plate under study reaches a stable flapping regime after approximately 25 flapping cycles, as indicated in Fig. 6, showing the flapping time-dependent behavior of the dimensionless drag and lift coefficients, respectively $C_D^* = C_D/C_{D,max}$ and $C_L^* = C_L/C_{L,max}$. Fig. 4 presents a phase portrait, the normalized transverse tip velocity of the plate, $U_x = V_x/U_\infty$, is plotted against the normalized transverse tip displacement, $X^* = x/L$. In Fig. 5 is shown the tip plate track in the X - Y plane. Fig. 8 shows the

Fast Fourier Transform (FFT) of the displacement amplitude in the frequency domain for FM3 mesh. Finally, Fig. 9 shows the envelope of the deformed configurations of the plate over one flapping period T , reporting the normalized displacements $X^* = x/L$ and $Y^* = y/L$.

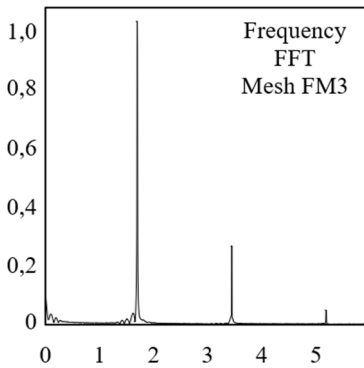


Fig. 8. Fast Fourier Transform in the frequency domain of the plate tip for mesh FM3

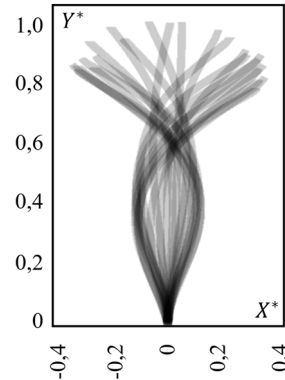


Fig. 9. Normalized displacement envelope during a flapping period T

5. Conclusions

This study presents selected results from ongoing research into the development of a fully open-source framework for analysing the interaction between fluids and highly flexible structures. A dynamic analysis of a thin plate subjected to FIV was performed in limit-cycle oscillation conditions. This allowed to characterise the spatiotemporal evolution of the flow field, and its correlation with the aerodynamic lift and drag coefficients. The present results are intended as a first numerical assessment of the framework, while quantitative validation against literature data for analogous configurations will be addressed in future work. Further work also will focus on investigating the potential of this approach for high fidelity engineering applications.

Acknowledgements

The authors have not disclosed any funding.

The authors would like to thank Dr. Pier Giuseppe Ledda of the Department of Civil and Environmental Engineering and Architecture of the University of Cagliari for his advice on fluid dynamics and for providing the computational resources to carry out the presented calculations.

Data availability

The datasets generated during and/or analyzed during the current study are available from the corresponding author on reasonable request.

Conflict of interest

The authors declare that they have no conflict of interest.

References

- [1] F. Lespagnol, C. Grandmont, P. Zunino, and M. A. Fernández, “A mixed-dimensional formulation for the simulation of slender structures immersed in an incompressible flow,” *Computer Methods in Applied Mechanics and Engineering*, Vol. 432, No. 117316, p. 117316, Dec. 2024, <https://doi.org/10.1016/j.cma.2024.117316>

- [2] E. A. Dowell and K. C. Hall, "Modeling of fluid-structure interaction," *Annual Review of Fluid Mechanics*, Vol. 33, pp. 445–490, 2001, <https://doi.org/10.1146/annurev.fluid.33.1.445>
- [3] F. Mazhar et al., "On the meshfree particle methods for fluid-structure interaction problems," *Engineering Analysis with Boundary Elements*, Vol. 124, pp. 14–40, Mar. 2021, <https://doi.org/10.1016/j.enganabound.2020.11.005>
- [4] Y. Bazilevs, K. Takizawa, and T. Tezduyar, *Computational fluid-structure interaction. Methods and applications*. Chichester, United Kingdom: John Wiley & Sons, Ltd, 2013.
- [5] Y. Yu, Y. Liu, and X. Amandolese, "A review on fluid-induced flag vibrations," *Applied Mechanics Reviews*, Vol. 71, No. 1, p. 010801, Jan. 2019, <https://doi.org/10.1115/1.4042446>
- [6] G. Hou, J. Wang, and A. Layton, "Numerical methods for fluid-structure interaction: a review," *Communications in Computational Physics*, Vol. 12, No. 2, pp. 337–377, 2015, <https://doi.org/10.4208/cicp.291210.290411s>
- [7] B. E. Griffith and N. A. Patankar, "Immersed methods for fluid-structure interaction," *Annual Review of Fluid Mechanics*, Vol. 52, No. 1, pp. 421–448, 2020, <https://doi.org/10.1146/annurev-fluid-010719-060228>
- [8] A. Nitti, J. Kiendl, A. Reali, and M. D. de Tullio, "An immersed-boundary/isogeometric method for fluid-structure interaction involving thin shells," *Computer Methods in Applied Mechanics and Engineering*, Vol. 364, No. 112977, p. 112977, Jun. 2020, <https://doi.org/10.1016/j.cma.2020.112977>
- [9] A. Nawafleh, T. Xing, V. Durgesh, and R. Padilla, "Fluid-structure interaction simulation of a flapping flag in a laminar jet," *Journal of Fluids and Structures*, Vol. 119, No. 103869, 2023, <https://doi.org/10.1016/j.jfluidstructs.2023.103869>
- [10] H. G. Weller, G. Tabor, H. Jasak, and C. Fureby, "A tensorial approach to computational continuum mechanics using object-oriented techniques," *Computers in Physics*, Vol. 12, No. 6, pp. 620–631, 1998, <https://doi.org/10.1063/1.168744>
- [11] G. Dhondt, *The Finite Element Method for Three-Dimensional Thermomechanical Applications*. Chichester, United Kingdom: Wiley, 2004, <https://doi.org/10.1002/0470021217>
- [12] G. Chourdakis et al., "preCICE v2: A sustainable and user-friendly coupling library," *Open Research Europe*, Vol. 2, No. 51, p. 51, Sep. 2022, <https://doi.org/10.12688/openreseurope.14445.2>